Optogenetic control of small GTPases reveals RhoA-mediated intracellular calcium signaling

Hironori Inaba[1,2], Qianqian Miao[1,2], Takao Nakata[1,2,3]

[1]Department of Cell Biology, Tokyo Medical and Dental University (TMDU), Bunkyo-ku, Tokyo, 113-8510, Japan.

[2]The Center for Brain Integration Research (CBIR), Tokyo Medical and Dental University (TMDU), Bunkyo-ku, Tokyo, 113-8510, Japan.

[3]Correspondence should be addressed to T.N. (E-mail: info.cbio@tmd.ac.jp)

Takao Nakata, M.D., Ph.D.

Department of Cell Biology, and The Center for Brain Integration Research (CBIR), Tokyo, Medical and Dental University (TMDU), 1-5-45 Yushima, Bunkyo-ku, Tokyo 113-8510, Japan.

TEL: +81-3-5803-5143

Running title: Optogenetic RhoA activation induces Ca^{2+} signaling

Abstract

Rho/Ras family small GTPases are known to regulate numerous cellular processes, including cytoskeletal reorganization, cell proliferation, and cell differentiation. These processes are also controlled by Ca^{2+}, and consequently, crosstalk between these signals is considered likely. However, systematic quantitative evaluation is not yet reported. Thus, we developed optogenetic tools to control the activity of small GTPases (RhoA, Rac1, Cdc42, Ras, Rap, and Ral) using an improved light-inducible dimer system (iLID). Using these optogenetic tools, we investigated calcium mobilization immediately after small GTPase activation. Unexpectedly, we found that only RhoA activation induced a transient intracellular calcium elevation in RPE1 and HeLa cells. Transients were also observed in MDCK and HEK293T cells by RhoA activation, but interestingly, molecular mechanisms were identified to be different among cell types. In RPE1 and HeLa cells, RhoA directly activated phospholipase C (PLC)ε at the plasma membrane, which in turn induced Ca^{2+} release from the endoplasmic reticulum (ER). The RhoA-PLCε axis induced calcium-dependent NFAT nuclear translocation, suggesting it does activate intracellular calcium signaling.

Introduction

Small GTPases of the Ras superfamily have been identified as molecular switches because they exist in two states, a GTP-binding state ("ON") and a GDP-binding state ("OFF") (Mitin et al., 2005; Wennerberg et al., 2005). These states are known to be regulated by activators – guanine nucleotide exchange factors (GEFs) – and inactivators, that is, GTPase-activating proteins (GAPs). Rho and Ras subfamily small GTPases localize at the plasma membrane (PM), respond to extracellular stimuli, and are responsible for a variety of biological processes, including cytoskeletal reorganization, cell proliferation, and cell differentiation (Mitin et al., 2005; Wennerberg et al., 2005). Several of these biological processes are also regulated by a universal second messenger, that is, calcium ion (Ca^{2+}) (Berridge et al., 2000; Clapham, 2007; Cullen and Lockyer, 2002). Thus, functional links must exist between these signaling pathways regulated by Rho/Ras family small GTPases and Ca^{2+}. Small GTPases and Ca^{2+} share some downstream factors that are coordinately regulated. For example, RhoA and Ca^{2+} regulate myosin II activity via myosin light chain phosphorylation (Amano et al., 1996; Ikebe and Hartshorne, 1985), and Ras and Ca^{2+} coordinate extracellular signal-regulated kinase (ERK)/mitogen-activated kinase (MAPK) signaling pathway (Chao et al., 1992; Kolch, 2000). Besides, small GTPases and Ca^{2+} are known to regulate each other's functions:

many GEFs and GAPs are regulated both positively and negatively by Ca^{2+} (Aspenström, 2004; Cullen and Lockyer, 2002), and some small GTPases regulate intracellular calcium signaling via activating phospholipase C (PLC) (Harden et al., 2009; Smrcka et al., 2012). PLC converts phosphatidylinositol 4,5-bisphosphate [$PI(4,5)P_2$] to two second messengers: diacylglycerol (DAG) and inositol-trisphosphate (IP_3). IP_3 reportedly binds to the IP_3 receptor (IP3R) to release Ca^{2+} from the endoplasmic reticulum (ER). This PLC-mediated calcium influx is the major calcium signaling pathway in non-excitable cells.

Despite the importance of crosstalk between small GTPases and intracellular calcium, details of the processes remain to be poorly understood. Especially, assessment of small GTPases' influences on intracellular calcium concentrations immediately after activation has been difficult because such activity could not be directly controlled in cells. However, optogenetics has changed this situation over the last decade.

Optogenetics is a pivotal tool for advancing cell biology because it enables control of specific signaling molecules at high spatiotemporal resolution both *in vitro* and *in vivo* (Guglielmi et al., 2016; Tischer and Weiner, 2014; Toettcher et al., 2011). Optogenetic control of small GTPases was first reported by Hahn's group (Wu et al., 2009). In the study, constitutively active mutants of Rac1 and Cdc42 were fused to the

blue-light-excited light-oxygen-voltage-sensing domain 2 (LOV2) of phototropin from *Avena sativa* (Christie et al., 1999). Photoactivatable (PA)–Rac1 and PA–Cdc42 were inactive in the dark due to steric hindrance of effector binding sites by the LOV2 domain. Blue-light irradiation made conformation changes to alpha-helix (Jα) that connects LOV2 domains to small GTPases, allowing them to bind effectors. However, this approach was difficult to optimize between "ON" and "OFF" states for other small GTPases. Therefore, PM translocation of their specific GEFs with light-induced heterodimeric systems, such as CRY2-CIBN (Kennedy et al., 2010), iLID (Guntas et al., 2015), TULIP (Strickland et al., 2012) and PhyB-PIF (Levskaya et al., 2009) systems, has been broadly used for regulating small GTPase activity including Rac1 (de Beco et al., 2018; Guntas et al., 2015; Levskaya et al., 2009), Cdc42 (de Beco et al., 2018; Guntas et al., 2015; Levskaya et al., 2009), RhoA (O'Neill et al., 2018; Valon et al., 2017; Wagner and Glotzer, 2016), Ras (Toettcher et al., 2013), and Ral (Zago et al., 2018).

We have developed optogenetic tools to control the activity of six members of the Rho and Ras subfamily GTPases (RhoA, Rac1, Cdc42, Ras, Rap, and Ral) by light-inducing GEF translocation to the PM using the iLID system. Using these optogenetic tools, we were able to examine small GTPase-mediated intracellular calcium mobilization for the first time. Unexpectedly, transient elevation of intracellular calcium concentrations

was only induced by optogenetic RhoA activation. These RhoA-mediated calcium transients were observed in all cell types examined, but the molecular mechanisms were different among the cell types. Furthermore, we found that RhoA directly activated PLCε in RPE1 and HeLa cells, which induced intracellular calcium signaling.

Results

Development of optogenetic tools for controlling small GTPase activity

Specific control of Rho/Ras family small GTPase activity at high spatiotemporal resolution was achieved using optogenetic tools. Among the several light-inducible heterodimerization systems, we chose the iLID system because of the reasons that follow: (1) it is based on the *As*LOV2 domain that can work without exogenously adding a chromophore to mammalian cells; (2) iLID-SspB heterodimerization can be controlled by blue-light with rapid on/off kinetics (seconds), which is suitable in controlling small GTPase activity at high spatiotemporal resolution; and (3) the molecular weight of proteins is small, allowing high-level expression in cells and relative ease of establishing a lentivirus vector for stable cell lines.

To evaluate the system, we developed an optogenetic tool to control RhoA activity (opto-RhoA; **Figure 1A**). Similar to previous studies (O'Neill et al., 2018; Valon et al., 2017; Wagner and Glotzer, 2016), a DH domain of the RhoA-specific GEF LARG (LARG-DH) was fused to SspB and fluorescence protein mVenus. The CAAX motif of K-Ras ($CAAX^{Kras}$) was fused to the C-terminus of iLID to localize on the PM. Further, the nuclear export signal (NES) was inserted between mVenus and SspB to avoid localizing to the nucleus, as originally reported (Guntas et al., 2015). Cells were

transfected with a single plasmid, mVenus-SspB-LARG-DH and iLID-CAAX^{KRas} linked with the cDNA of the self-cleaved P2A peptide. In the dark, mVenus-SspB-LARG-DH was diffusely localized in the cytoplasm (**Figure 1B, 458 nm light OFF**). Blue-light irradiation with a 458 nm laser has induced iLID-SspB heterodimerization, which in turn translocated LARG-DH to the PM where it could activate RhoA (**Figure 1B, 458 nm light ON**). RhoA activation by opto-RhoA was tested using a RhoA activity reporter: mCherry fused Rho-binding domain derived from the RhoA-specific effector Rhotekin (mCherry-RBD$_{Rhotekin}$) (Reid et al., 1996). Opto-RhoA and mCherry-RBD$_{Rhotekin}$ were transfected into HeLa cells, and cells were locally irradiated with a 458 nm laser (**Figure 1C and Movie 1**). During irradiation, mVenus-SspB-LARG-DH rapidly accumulated in the irradiated area, while mCherry-RBD$_{Rhotekin}$ did so, however, in a gradual manner (**Figure 1D**). Accumulation disappeared after irradiation was terminated. These data suggest that RhoA activity can be controlled spatiotemporally using the opto-RhoA as previously reported (O'Neill et al., 2018; Valon et al., 2017; Wagner and Glotzer, 2016).

We next developed optogenetic tools for another five members of Rho and Ras family GTPases (Rac1, Cdc42, Ras, Rap, and Ral) implicated in regulating intracellular calcium signaling (Harden et al., 2009; Smrcka et al., 2012) (**Supplementary Figure 1**). The LARG-DH of opto-RhoA was replaced with GEF domains of specific GEFs for each

small GTPase (see details in the Materials and Methods section); most were already reported for application in optogenetic tools (Guntas et al., 2015; Toettcher et al., 2013; Zago et al., 2018). We termed these optogenetic tools as opto-X (X: target GTPases).

Screening using opto-GTPases for induction of changes in intracellular calcium concentrations

We monitored changes of intracellular calcium concentrations with a genetically encoded red fluorescent calcium indicator R-GECO1 that is known to detect physiological calcium changes as found during neural activity and muscle contraction (Zhao et al., 2011). Opto-GTPases and the calcium reporter R-GECO1 were transfected into human non-transformed (RPE1) and cancer (HeLa) cells. Changes of intracellular calcium concentrations induced by persistent activation of small GTPases were observed via confocal microscopy. Only RhoA was identified to induce transient elevation of intracellular calcium concentrations both in RPE1 and HeLa cells **(Figure 2, Supplementary Figure 2, and Movie 2)**. We also tested a YA mutant of opto-RhoA (opto-RhoA^{YA}) that possessed a LARG Y940A mutation that abolished GEF activity (Martz et al., 2013). Opto-RhoA^{YA} rarely induced calcium transients (1 out of 136 RPE1 cells and 0 out of 133 HeLa cells; **Figure 2C**), confirming that calcium transients were

induced by RhoA activation and not by blue-light irradiation or by photoswitch translocation to the PM.

Further, we examined RhoA-mediated calcium transients in MDCK and HEK293T cells. These cells also exhibited the calcium transients immediately after RhoA activation (30 % and 41 % of cells in MDCK (n = 50) and HEK293T (n = 52) cells, respectively; **Supplementary Figure 2 and Movie 2**). Thus, all cells examined exhibited RhoA-mediated calcium transients. Of note, membrane blebbing, produced by actomyosin-mediated cellular contraction induced by RhoA activation (Charras et al., 2005), was seen in opto-RhoA-transfected HEK293T cells even before blue-light irradiation (**Supplementary Figure 2 and Movie 2**). This observation suggests that opto-RhoA was somewhat leaky, that is, opto-RhoA exerts background activity in the dark. The number of blebs was dramatically increased after the blue-light irradiation, indicating that the blue-light irradiation did increase RhoA activity.

Time-course analysis showed that initiation of an increase in intracellular calcium concentration was observed within 10 seconds in RPE1, HeLa, and HEK293T cells; meanwhile, maximum concentration was observed about 20 seconds after light irradiation (**Figure 2D**). In contrast, initiation of this increase was observed within 20–30 seconds, and the maximum increase was reached about 2 minutes after light irradiation

in MDCK cells (**Figure 2D**). Cellular responses differed among cell types.

Mechanisms of RhoA-induced calcium transients are different among cell types

We investigated molecular mechanisms of RhoA-induced intracellular calcium transients using small molecule inhibitors (see **Figure 7** for summary). Several calcium channels are activated by RhoA and its downstream factors (Li and Brayden, 2017; Mehta et al., 2003; Wing et al., 2003). We initially examined the RhoA-ROCK-myosin II axis, the major pathway of the RhoA signaling pathway. Both ROCK inhibitor, Y-276322, and myosin II inhibitor, Blebbistatin, were observed to efficiently inhibit RhoA-induced calcium transients in MDCK and HEK293T cells, but surprisingly not in RPE1 and HeLa cells (**Figure 3**). Actomyosin-mediated cellular contraction activates mechanosensitive (MS) calcium channels such as Piezo1 and transient receptor potential (TRP) family channels in MDCK and HEK293T cells.

Further, we tested the non-selective calcium channel blockers SKF96365 and 2-APB (**Figure 3**). SKF96365 was observed to inhibit the RhoA-induced calcium transients in MDCK and HEK293T cells (**Figures 3C, D**). Conversely, 2-APB blocked transients in RPE1 and HeLa cells (**Figures 3A, B**). Mechanisms of RhoA-induced calcium transients are clearly different among cell types. Our further studies focused on molecular

mechanisms of RhoA-induced calcium transients in RPE1 and HeLa cells.

RhoA-PLCε axis induces calcium transients in RPE1 and HeLa cells

2-APB inhibits IP3R, and RhoA directly activates a PLC isoform PLCε (Wing et al., 2003). Thus, we hypothesized that the RhoA-PLCε axis has induced calcium transients in RPE1 and HeLa cells; we also further examined the effect of the PLC inhibitor U73122 **(Figures 3A, B)**. Initially, calcium transients were not affected by U73122 in L-15 medium. However, U73122 is reported to spontaneously form conjugates with chemical components of cell culture medium, such as L-glutamine, glutathione, and bovine serum albumin (BSA). This conjugation causes loss of inhibitory activity toward PLC (Wilsher et al., 2007). Calcium transients were abolished by U71322 both in RPE1 and HeLa cells in this condition when incubated in Ringer's solution. As hypothesized, RhoA activates PLC, which in turn induces calcium transients.

We also tested RhoA-induced calcium transients in calcium-free buffers (**Figures 3A, B**). The percentage of cells exhibiting calcium transients significantly decreased in both cell types. However, about 10 % of cells still showed transients, and intracellular calcium stores have been identified as a source of these calcium transients. Extracellular calcium could be required for proper calcium homeostasis.

We also knocked down PLCε in RPE1 and HeLa cells with small interference RNA (siRNA) and examined calcium transients (**Figures 4A, B**). Blue-light irradiation of PLCε-depleted cells did not induce calcium transients. Further, ECFP-fused mouse PLCε (msPLCε), not ECFP alone, rescued calcium transient phenotypes in PLCε-depleted cells (**Figures 4C–E, Supplementary Figure 3**). PLCε is thus essential for calcium transients induced by RhoA in RPE1 and HeLa cells.

We performed additional rescue experiments with several PLCε mutants in PLCε-depleted HeLa cells to further confirm the RhoA-PLCε functions. PLCε displays a lipase domain that includes a PH domain, four EF-hand domains, a catalytic core X-Y domain, and a C2 domain and also a CDC25 homology domain which activates Rap1 (Citro et al., 2007; Jin et al., 2001; Lopez et al., 2001) (**Figure 4C**). This information led us to examine the function of PLCε essential for RhoA-induced calcium transients. The GEF-inactive mutant, F702A PLCε, which corresponds to the F929A GEF-inactive mutant of a RasGEF SOS (Hall et al., 2001), has rescued calcium phenotype in PLCε-depleted cells. Conversely, the lipase-inactive mutant, H1433L (Lopez et al., 2001), did not rescue the phenotype (**Figures 4D, E**). Lipase activity appears essential for calcium transients.

PLCε is also regulated by Ras (Kelley et al., 2001; Song et al., 2001), Rap1 (Jin

et al., 2001), Ral (Kelley et al., 2004), and heterotrimeric G-protein β and γ subunits ($G_{\beta\gamma}$) (Wing et al., 2001). A unique insert in the Y domain (Yins in **Figure 4C**) of PLCε is required for its activation by RhoA (Wing et al., 2003). In contrast, Ras and Rap1 are seen to bind directly to the second Ras association domain (RA2 domain in **Figure 4C**) (Bunney et al., 2006) of PLCε. Then, we performed rescue experiments in PLCε-depleted HeLa cells with a Yins-deleted PLCε mutant (ΔYins) and the R2130L PLCε mutant which abolishes interactions with Ras (Bunney et al., 2006) (**Figure 4D**). As a result, the R2130L mutant rescued the calcium phenotype in PLCε-depleted cells, but the ΔYins mutant did not (**Figure 4E**). RhoA directly activates the phospholipase activity of PLCε, which in turn induces intracellular calcium transients.

RhoA activation at the PM but not in the Golgi is essential for the calcium transients

PLCε was recently reported to be activated at the Golgi, and not at the PM in cardiac cells, to hydrolyze phosphatidylinositol 4-phosphate [PI(4)P] (Malik et al., 2015; Nash et al., 2019; Zhang et al., 2013). Our optogenetic system, iLID-CAAX^{KRas}, largely localizes to the PM but is also partially localized in the Golgi. Thus, opto-RhoA could activate Golgi RhoA. However, PI(4)P hydrolysis produces inositol bisphosphate (IP_2) but not IP_3, and PLCε activation at the Golgi is not likely to induce IP3R-dependent calcium release from

the ER. We examined this issue by constructing opto-RhoA-TGN (*trans*-Golgi network) using an N-terminus transmembrane domain of 2,6-sialyltransferase (Shiwarski et al., 2017), and opto-RhoA-Golgi with KDELr D193N dominant-negative mutant (KDELr DN) (Irannejad and Wedegaertner, 2010), instead of the $CAAX^{KRas}$ motif (**Figures 5A, B**). Both in RPE1 and HeLa cells, only about 10 % of cells expressing opto-RhoA-TGN exhibited calcium transients, and cells expressing opto-RhoA-Golgi did not (**Figure 5C**). RhoA activation at the PM appears essential for calcium transients.

We next explored $PI(4,5)P_2$ dynamics on the PM using the $PI(4,5)P_2$ marker, a PH domain of PLCδ (PLCδ-PH) (Stauffer et al., 1998) and an optogenetic tool for controlling the inositol 5-phosphatase (opto-5-ptase) with the inositol 5-phosphatase domain of OCRL ($OCRL_{cat}$) and the CRY2-CIBN heterodimerization system, as previously reported (Idevall-Hagren et al., 2012) (**Figure 5D**). This latter construct served as a positive control. CRY2-CIBN heterodimerization is induced by blue-light irradiation. Cytosolic ECFP-CRY2-$OCRL_{cat}$ then translocates to the PM in functional form. When 5-phosphatase was recruited to the PM, the fluorescence intensity of cytosolic mCherry-PLCδ-PH increased to about 40 % within 30 seconds (**Figures 5E, F and Movie 3)**, indicating that membrane $PI(4,5)P_2$ decreased. In contrast, when RhoA was activated by opto-RhoA, the intensity of cytosolic mCherry-PLCδ-PH increased only about 10 % even

after 5 minutes. This result is comparable to intensity changes of mCherry alone (**Figures 5E, F and Movie 4**). RhoA-mediated cellular contraction might also cause this increase of mCherry intensity since we quantified mCherry intensity in a constant square area. The RhoA-PLCε axis functions at the PM, but only marginally affects membrane phosphoinositide dynamics.

RhoA-PLCε axis induces calcium signaling

Finally, we examined RhoA-PLCε-mediated intracellular calcium transients for activation of intercellular calcium signaling with an NFAT nuclear translocation assay. NFAT is identified as a transcription factor, and, after dephosphorylation by calmodulin-calcineurin, it translocates from the cytoplasm to the nucleus (Hogan et al., 2003). About 30 % of cells exhibited mCherry-NFAT nuclear translocation after RhoA activation with opto-RhoA (**Figures 6A, B, and Movie 5**). This response is comparable to the percentage of cells that exhibited calcium transients. Translocation was abolished by treatment with PLCε-specific siRNA (**Figures 6C, D**), indicating that the RhoA-PLCε axis induces intracellular calcium signaling.

Discussion

In this study, we have developed optogenetic tools to control Rho and Ras family GTPase activity; we then performed cell-based systematic functional screening (**Figure 2**). We focused on intracellular calcium signaling induced by Rho and Ras signaling. This approach for cell-based screening is applicable for other signaling pathways as well if both optogenetic tools and biosensors are available. Before the introduction of optogenetic tools, single cell-based enzymology was difficult due to the lack of sufficient spatiotemporal resolution and specificity. Optogenetics has resolved this issue by exerting control over specific signaling molecules using a light stimulus with high spatiotemporal resolution. This tool provides a powerful platform for cell-based enzymology.

Surprisingly, only RhoA activation was seen to induce calcium transients in screening using opto-GTPases (**Figure 2**); other GTPases are also reported to induce calcium signaling (Harden et al., 2009; Smrcka et al., 2012). The sensitivity of our experiments may not have been sufficient to detect calcium transients by such GTPase activation, or leaks in our optogenetic systems (**Supplementary Figure 2**) may have affected signaling responses. However, RhoA activation has induced calcium transients under the same conditions. Another possibility is that activation of only individual small GTPases does not induce calcium transients. Other signals, such as PI3K, could be

required for activating calcium signaling. Our study is the first to induce temporal activation of specific GTPases and monitor subsequent changes of intracellular calcium. This approach is expected to have much higher specificity and time resolution compared with previous studies. Further, our systems can simultaneously stimulate other signals using multiple optogenetic tools, and we can examine dual activation of small GTPases and other signals for induction of calcium transients. Such experiments could explain many discrepancies in signal transduction.

RhoA-induced calcium transients were observed in all cell lines examined in this study (**Figure 2 and Supplementary Figure 2**) and have also been reported previously in still other cell lines (Li and Brayden, 2017; Mehta et al., 2003; Wing et al., 2003). RhoA appears to generally induce calcium signaling. However, only up to about 50 % of cells expressing opto-RhoA show calcium transients. This observation could be explained in part by transfection-related issues, such as damage to cells. There were cells with varying levels of the expression of opto-RhoA and R-GECO1. Most of the cells with high expression of opto-RhoA and/or R-GECO1 did not show calcium transients, suggesting that the overproduction of exogenous proteins could be cytotoxic. Also, such high expression could cause RhoA activation even in the dark, with concomitant background effects. However, there were still cell populations that appeared healthy, did not highly

express exogenous proteins, but still did not exhibit calcium transients.

RhoA-induced calcium transients might also be dependent on cellular contexts, such as cell-cycle stage; expression and posttranslational modifications of downstream molecules, including RhoA and PLCε; and intracellular calcium concentrations. Most importantly, almost all cells initially exhibited calcium transients also responded repeatedly to blue-light irradiation after a few minutes of rest (data not shown), ensuring reproducibility of RhoA-mediated calcium transients.

Unexpectedly, molecular mechanisms underlying calcium transients were found to be notably different among cell types (**Figures 3, 7**). In MDCK and HEK293 cells, the RhoA-ROCK-Myosin II axis induced calcium transients (**Figures 3C, D**). Actomyosin-mediated contractile force is also reported to induce membrane tension changes that activate MS channels (Jin et al., 2020) (**Figure 7, lower scheme**). One candidate is the Piezo channel that is reported in both MDCK (Gudipaty et al., 2017) and HEK293T cells (Cox et al., 2016). However, Piezo channel is not sensitive to SKF96365 (Weng et al., 2018), which inhibited transient induction (**Figures 3C, D**). Thus, other MS calcium channels, such as a member of the TRP family of channels, may be needed for RhoA-induced calcium transients. Further studies are also required to elucidate molecular mechanisms for the RhoA-ROCK-Myosin II-mediated calcium transients.

In contrast, the RhoA-PLCε axis was determined to be functional in RPE1 and HeLa cells (**Figures 3, 4 and 7, upper scheme**). Calcium transients were totally blocked by 2-APB and partially observed in Ca^{2+}-free buffer, and transients were apparently induced by the IP_3-IP3R pathway that promotes Ca^{2+} release from the ER. In the Ca^{2+}-free buffer, the percentage of cells exhibiting transients has decreased compared with cells in Ca^{2+}-containing buffer. This finding may reflect changes in cellular responsiveness since cell processes, such as cell-substrate adhesion, membrane lipid composition, and intracellular calcium homeostasis, are largely dependent on extracellular Ca^{2+}, for example, purified PLCε exhibits Ca^{2+}-dependent phospholipase activity (Kelley et al., 2001).

PLCε has been identified to be activated by other small GTPases, including Ras, Rap, and Ral (Jin et al., 2001; Kelley et al., 2004, 2001), which is inconsistent with the present results (**Figure 2**). This discrepancy is explained by the fact that there is no evidence that small GTPases directly activate the PLCε. In previous studies, phospholipase activity was typically examined by IP_3 accumulation in COS-7 cells co-expressing constitutively active mutants of small GTPases and PLCε exogenously (Ada-Nguema et al., 2006; Kelley et al., 2004, 2001; Madukwe et al., 2018; Martins et al., 2012; Wing et al., 2003). This assay cannot exclude side effects of Ras signaling. Also,

the purified KRas G12V constitutively active mutant activated phospholipase activity of N-terminal deleted PLCε (Seifert et al., 2008), but did not that of the full-length intact PLCε (Song et al., 2001) in an *in vitro* reconstitution assay. Active Ras and Rap likely interact with the RA2 domain of PLCε and induce translocation from cytoplasm to the PM and Golgi, respectively (Jin et al., 2001; Song et al., 2001). Thus, PLCε is identified as an effector protein of Ras and Rap GTPases, but this present study suggests that Ras and Rap do not directly activate its phospholipase activity. Instead, other factors, including RhoA, activate PLCε that is recruited to the membrane by Ras and Rap (Bunney et al., 2006). We attempted to determine whether RhoA also recruits PLCε to the PM, but definitive results were not obtained. However, membrane targeting for PLCε with the CAAX motif is required for RhoA-dependent activation for RA2 domain-depleted PLCε (Madukwe et al., 2018), and membrane recruitment of PLCε by RA2 domain-interacting proteins, Ras and Rap, could be necessary for activation by RhoA. Yins of PLCε are required for RhoA-dependent activation, yet the Y domain does not interact with RhoA (Wing et al., 2003). A recent study has reported that RhoA interacted with the PH and RA1-RA2 domains of PLCε (Yu et al., 2020). However, further studies are needed to understand molecular mechanisms of PLCε activation by RhoA, including whether translocation of PLCε by Ras or Rap1 is essential.

We have shown that RhoA-mediated calcium transients induce NFAT translocation to the nucleus (**Figure 6**). NFAT translocation was used because of ease of assess, but little is known about the physiological function of the RhoA-NFAT pathway (Henstidge et al., 2009; Xu et al., 2004; Zhu et al., 2013). Instead, our findings indicate that the RhoA-induced calcium transients activate intracellular calcium signaling. Both RhoA and calcium signaling commonly regulate actin cytoskeleton reorganization, cell proliferation, and gene expression (Berridge et al., 2000; Bong and Monteith, 2018; Clapham, 2007; Cullen and Lockyer, 2002; Heasman and Ridley, 2008), and coordination of signaling seems reasonable. To date, upstream factors and physiological roles of RhoA-PLCε have been reported in a few cell types including kidney podocytes (Kalwa et al., 2015; Yu et al., 2020), astrocytes (Citro et al., 2007), and cardiac cells (Xiang et al., 2013). PLC activates not only calcium signaling but also DAG-PKC signaling. Such signaling reportedly affects various cellular pathways, and physiological roles of the RhoA-PLCε axis may be different among cell types. This axis should be examined in more cell types in the future.

Materials and Methods

Antibodies

Commercial antibodies and their dilution were indicated as follows; mouse anti-GFP antibody diluted at 1:1000 (clone mFX75, FUJIFILM Wako Pure Chemical Corp., Osaka, Japan); anti-vinculin antibody diluted at 1:1000 (clone 2B5A7, Proteintech Group, Chicago, IL); rabbit anti-PLCE1 antibody diluted at 1:1000 (HPA015597, Atlas Antibodies, Bromma, Sweden); peroxidase-conjugated mouse anti-β-actin antibody diluted at 1:10000 (clone 2F3, FUJIFILM Wako Pure Chemical Corp.); peroxidase-conjugated sheep anti-mouse IgG antibody diluted in 1:4000 (NA931, GE Healthcare, Little Chalfont, UK); and peroxidase-conjugated donkey anti-rabbit IgG antibody diluted in 1:2000–1:4000 (NA934, GE Healthcare).

Cell culture and transfection

hTERT-immortalized human retinal pigment epithelial (RPE1) cells (ATCC CRL-400) were cultured in DMEM and F12 nutrient mix (1:1), supplemented with 10 % (v/v) fetal bovine serum (FBS: Biowest, Nuaillé, France). HeLa (RCB0007: RIKEN BRC through the National BioResource Project of the MEXT/AMED, Japan), MDCK (kindly gifted from Dr. N. Yui), and HEK293T (obtained from TaKaRa, Shiga, Japan) cells were

cultured in DMEM supplemented with 10 % FBS. Plasmid transfection was performed using Lipofectamine™ 2000 (Thermo Fisher Scientific, Waltham, MA) following the manufacturer's instructions. Reagents were obtained from commercial sources as follows: Y-27632 dihydrochloride (Focus, Biomolecules, Plymouth Meeting, PA); (-)-Blebbistatin (Cayman Chemical, Ann Arbor, MI); U73122 (Cayman Chemical); 2-APB (FUJIFILM Wako Pure Chemicals); and SKF96365 (FUJIFILM Wako Pure Chemicals).

DNA construction

pLL7.0: Venus-iLID-CAAX (from KRas4B) and pLL7.0: tgRFPt-SSPB wild-type (WT) (Guntas et al., 2015) were gifts from Brian Kuhlman (Addgene plasmid #60411 and #60415); PR_GEF (2XPDZ-mCherry-Larg (DH)) from Michael Glotzer (Addgene plasmid #80407); CMV-R-GECO1 (Kalko et al., 2011) from Robert Campbell (Addgene plasmid #32444); pcDNA3-HA-human OCRL (Erdmann et al., 2007) from Pietro De Camilli (Addgene plasmid #22207); GFP-C1-PLCdelta-PH (Stauffer et al., 1998) from Tobias Meyer (Addgene plasmid #21179); pTriEx-RhoA FLARE.sc Biosensor WT (Pertz et al., 2006) from Klaus Hahn (Addgene plasmid #12150); and human C3G cDNA from Hiroki Tanaka (Kyoto University). HA-NFAT1(1-460)-mCherry was constructed previously (Ishii et al., 2015). Total RNA was obtained from RPE1 and HeLa cells using

QIAzol Lysis Reagent (QIAGEN; Hilden, Germany) following the manufacturer's protocol, and first-strand cDNA was synthesized with 1 μg total RNA using a SuperScript III First-Strand Synthesis System for RT-PCR (TaKaRa) following the manufacturer's protocol.

msPLCε cDNA was amplified by PCR from mouse liver first-strand cDNA library (kindly gifted from Tomohiro Ishii) using Tks Gflex polymerase (TaKaRa) and was cloned between *Nhe*I and *Kpn*I sites of pECFP-N1 (Clontech, Palo Alto, CA). msPLCε sequences were sensitive to siPLCε seq1, and a siRNA-resistant msPLCε mutant was used in this study. All point mutations were generated using site-directed mutagenesis methods by Tks Gflex polymerase. msPLCε ΔYins mutant was generated with overlap extension PCR.

To create pmCherry-PLCδ-PH, EGFP was removed from pEGFP-C1 PLCdelta-PH and replaced with mCherry from pmCherry-C1 (TaKaRa). To create pmCherry-C1 $RBD_{rhotekin}$, $RBD_{rhotekin}$ was amplified from pTriEx-RhoA FLARE.sc Biosensor WT and cloned between *Bgl*II and *Eco*RI site of pmCherry-C1.

Then, the DNA coding sequence was cloned between *Nhe*1 and *Not*1 of pEGFP-N1 to create opto-RhoA (mVenus-NES-SspB-LARG-DH-P2A-iLIDcaax). The NES sequence (FGIDLSGLTL) was directly linked to mVenus. SspB and LARG-DH (DH

domain of LARG, aa 766–986) were linked by LDSAGGSAGGSAGGLE. The P2A peptide sequence (GSG)ATNFSLLKQAGDVEENPGP was directly linked to LARG-DH and followed by the linker APGS to locate the 2A product protein to the precise subcellular domain (Kakumoto and Nakata, 2013).

The transmembrane domain of 2,6-sialyltransferase (aa 1–32) was then amplified from the HeLa cDNA library to create opto-RhoA-TGN, and KDELr was amplified from the RPE1 cDNA library by PCR to create opto-RhoA-Golgi. These fragments were connected to iLID by overlap extension PCR with a GSGSGS (3×GS) linker. iLID-KDELr was first cloned into a pECFP-C1 vector (Clontech), and KDELr D193N dominant-negative mutant (KDELr DN) was then generated by site-directed PCR. iLID-CAAX^{Kras} of opto-RhoA was replaced with iLID-TGN or iLID-KDELr DN.

The LARG-DH of opto-RhoA was replaced with a DH-PH domain of Tiam (Tiam-DH-PH, aa 1012–1591), a DH-PH domain of ITSN (ITSN-DH-PH, aa 1230–1580), a catalytic domain of SOS2 (SOS2cat, aa 563–1048), a catalytic domain of C3G (C3Gcat, aa 687–1077), and a GEF domain of RGL2 (RGL2-GEF, aa 1–518) to create opto-Rac1, -Cdc42, -Ras, -Rap1, and -RalA/B, respectively.

Opto-5-ptase was constructed as previously reported for mCherry-PHR-iSH-2A-CIBNcaax (Kakumoto and Nakata, 2013), in which the vector backbone was changed to

pEGFP-N1, and mCherry and iSH were replaced with ECFP and the inositol 5-phosphate domain of OCRL (OCRLcat, aa 234–539), respectively.

All cloned fragments were verified by sequencing.

Small interference RNAs

Transfection of siRNA duplexes used Lipofectamine™ RNAiMAX reagent following the manufacturer's protocol (Thermo Fisher Scientific). Each duplex was used at a final concentration of 10 nM. Double-strand RNAs were purchased from Ambion, Thermo Fisher Scientific. Target nucleotide sequences were 5′–GCAAGGAGCTGATCGATCT–3′ (s27658, siPLCε seq1), 5′–GGACATAGGCTGACAACCA–3′ (s27659, siPLCε seq2), and 5′–TACTGCGATATTGAAGTCC–3′ (s27660, siPLCε seq3), respectively. #2 siRNA (Silencer Select, Thermo Fisher Scientific) was used as a negative control.

Live cell imaging

When only the plasmid transfection was performed, cells were seeded on glass-bottomed dishes (Greiner Bio-one, Kremsmünster, Austria) coated with collagen (Cellmatrix Type IC; Nitta Gelatin Inc., Osaka, Japan) 2 days before the observations. On the next day, cells were transfected with the plasmid and were analyzed a day later. When both siRNA

and plasmid transfection were performed, cells were seeded 3 days before the observations. On the next day, siRNA transfection was performed. After 24 hours since siRNA transfection, plasmid transfection was performed, and cells were analyzed a day later. Before experiments, the medium was changed to Leibovitz's L-15 (Thermo Fisher Scientific), Ringer's solution (138 mM NaCl, 5.6 mM KCl, 2mM $CaCl_2$, 2 mM $MgCl_2$, 4 mM D-glucose, 5 mM HEPES, and 2 mM sodium pyruvate (pH 7.4, adjusted with NaOH)), or calcium-free Ringer's solution (sans $CaCl_2$). Cells were analyzed under serum-starved conditions, and a closed heated chamber was used during live cell imaging at 37 °C without CO_2. Images were obtained with a confocal laser scanning microscope (FV1200, Olympus, Tokyo, Japan) on an IX83 microscope (Olympus) equipped with 40×/0.95 NA and 20×/0.7 NA dry objective lenses and FV10-ASW software (Olympus). A laser line (458 nm) was used to photo-activated photoswitches. Local irradiation was performed using multi-area time-lapse software (Olympus). Image analysis used ImageJ/Fiji software (NIH) (Schindelin et al., 2012). Adobe Illustrator CS6 (Adobe Systems, San Jose, CA) was used for final figure preparation.

Immunoblotting

Cells were lysed with 2 × SDS sample buffer (125 mM Tris-HCl (pH6.8), 4 % (w/v) SDS,

10 % (w/v) sucrose, 0.01 % (w/v) BPB, 5 % (v/v) 2-mercaptoethanol). Proteins were separated with SDS-PAGE and then later transferred to PVDF membranes by electrophoresis using a Bio-Rad Trans-Blot device (Bio-Rad, Richmond, CA). Blots were blocked for an hour at room temperature or overnight at 4 °C with 5 % skim milk in Tris-buffer saline with Tween-20 (TBS-T, 50 mM Tris-HCl (pH 7.4), 138 mM NaCl, 2.7 mM KCl, and 0.1 % (v/v) Tween-20). Membranes were washed with TBS-T and incubated with indicated antibodies diluted in Can Get Signal Solution 1 (TOYOBO, Osaka, Japan) for 1 h at room temperature. Membranes were washed in TBS-T, incubated with appropriate horseradish peroxidase-conjugated secondary antibodies diluted in Can Get Signal Solution 2 (TOYOBO) for 1 h at room temperature, and washed again in TBS-T. Blots were developed with ImmunoStar Zeta (FUJIFILM Wako Pure Chemical), and chemiluminescence signals were visualized via a ChemiDoc MP system (Bio-Rad).

Statistics

Statistical analyses were performed using Excel (Microsoft) and R software v.3.5.1 (R Development Core Team, 2016). All graphs were drawn using Excel software.

Acknowledgments

The authors are grateful to Dr. Naofumi Yui (TMDU) for the kind gift of MDCK cells and Toshiyuki Kakumoto for plasmid construction. We also thank Drs. Tomohiro Ishii and Toshifumi Asano for the helpful discussion and Satoko Nakamura for secretarial expertise.

Funding

This work was supported in part by JSPS KAKENHI (18K15002 and 20K16105 to H.I., and 18K19328 to H.I. and T.N.), by Research Grants from the Takeda Science Foundation (to H.I.), and the Kanehara Ichiro Memorial Foundation (to H.I.).

Authors' contributions

H.I. and T.N. designed the experiments and wrote the manuscript. H.I. and Q.M. performed the experiments, and H.I. analyzed the data.

Conflict of interests

The authors declare that they have no conflict of interests.

References

Ada-Nguema AS, Xenias H, Sheetz MP, Keely PJ. 2006. The small GTPase R-Ras regulates organization of actin and drives membrane protrusions through the activity of PLCε. *J Cell Sci*. doi:10.1242/jcs.02835

Amano M, Ito M, Kimura K, Fukata Y, Chihara K, Nakano T, Matsuura Y, Kaibuchi K. 1996. Phosphorylation and activation of myosin by Rho-associated kinase (Rho-kinase). *J Biol Chem*. doi:10.1074/jbc.271.34.20246

Aspenström P. 2004. Integration of signalling pathways regulated by small GTPases and calciumBiochimica et Biophysica Acta - Molecular Cell Research. doi:10.1016/j.bbamcr.2004.09.029

Berridge MJ, Lipp P, Bootman MD. 2000. The versatility and universality of calcium signalling. *Nat Rev Mol Cell Biol*. doi:10.1038/35036035

Bong AHL, Monteith GR. 2018. Calcium signaling and the therapeutic targeting of cancer cells. *Biochim Biophys Acta - Mol Cell Res*. doi:10.1016/j.bbamcr.2018.05.015

Bunney TD, Harris R, Gandarillas NL, Josephs MB, Roe SM, Sorli SC, Paterson HF, Rodrigues-Lima F, Esposito D, Ponting CP, Gierschik P, Pearl LH, Driscoll PC, Katan M. 2006. Structural and mechanistic insights into ras association domains of

1 phospholipase C epsilon. *Mol Cell*. doi:10.1016/j.molcel.2006.01.008

2 Chao TSO, Byron KL, Lee KM, Villereal M, Rosner MR. 1992. Activation of MAP

3 kinases by calcium-dependent and calcium-independent pathways. Stimulation by

4 thapsigargin and epidermal growth factor. *J Biol Chem*.

5 Charras GT, Yarrow JC, Horton MA, Mahadevan L, Mitchison TJ. 2005. Non-

6 equilibration of hydrostatic pressure in blebbing cells. *Nature* **435**:365–369.

7 doi:10.1038/nature03550

8 Christie JM, Salomon M, Nozue K, Wada M, Briggs WR. 1999. LOV (light, oxygen, or

9 voltage) domains of the blue-light photoreceptor phototropin (nph1): Binding sites

10 for the chromophore flavin mononucleotide. *Proc Natl Acad Sci U S A* **96**:8779–

11 8783. doi:10.1073/pnas.96.15.8779

12 Citro S, Malik S, Oestreich EA, Radeff-Huang J, Kelley GG, Smrcka A V., Brown JH.

13 2007. Phospholipase Cε is a nexus for Rho and Rap-mediated G protein-coupled

14 receptor-induced astrocyte proliferation. *Proc Natl Acad Sci U S A* **104**:15543–

15 15548. doi:10.1073/pnas.0702943104

16 Clapham DE. 2007. Calcium Signaling. *Cell*. doi:10.1016/j.cell.2007.11.028

17 Cox CD, Bae C, Ziegler L, Hartley S, Nikolova-Krstevski V, Rohde PR, Ng CA, Sachs

18 F, Gottlieb PA, Martinac B. 2016. Removal of the mechanoprotective influence of

the cytoskeleton reveals PIEZO1 is gated by bilayer tension. *Nat Commun*. doi:10.1038/ncomms10366

Cullen PJ, Lockyer PJ. 2002. Integration of calcium and Ras signalling. *Nat Rev Mol Cell Biol*. doi:10.1038/nrm808

de Beco S, Vaidžiulytė K, Manzi J, Dalier F, di Federico F, Cornilleau G, Dahan M, Coppey M. 2018. Optogenetic dissection of Rac1 and Cdc42 gradient shaping. *Nat Commun*. doi:10.1038/s41467-018-07286-8

Erdmann KS, Mao Y, McCrea HJ, Zoncu R, Lee S, Paradise S, Modregger J, Biemesderfer D, Toomre D, De Camilli P. 2007. A Role of the Lowe Syndrome Protein OCRL in Early Steps of the Endocytic Pathway. *Dev Cell* **13**:377–390. doi:10.1016/j.devcel.2007.08.004

Gudipaty SA, Lindblom J, Loftus PD, Redd MJ, Edes K, Davey CF, Krishnegowda V, Rosenblatt J. 2017. Mechanical stretch triggers rapid epithelial cell division through Piezo1. *Nature*. doi:10.1038/nature21407

Guglielmi G, Falk HJ, De Renzis S. 2016. Optogenetic Control of Protein Function: From Intracellular Processes to Tissue Morphogenesis. *Trends Cell Biol* **26**:864–874. doi:10.1016/j.tcb.2016.09.006

Guntas G, Hallett RA, Zimmerman SP, Williams T, Yumerefendi H, Bear JE, Kuhlman

1 B. 2015. Engineering an improved light-induced dimer (iLID) for controlling the
2 localization and activity of signaling proteins. *Proc Natl Acad Sci U S A* **112**:112–
3 117. doi:10.1073/pnas.1417910112
4 Hall BE, Yang SS, Boriack-Sjodin PA, Kuriyan J, Bar-Sagi D. 2001. Structure-based
5 Mutagenesis Reveals Distinct Functions for Ras Switch 1 and Switch 2 in Sos-
6 catalyzed Guanine Nucleotide Exchange. *J Biol Chem*.
7 doi:10.1074/jbc.M101727200
8 Harden TK, Hicks SN, Sondek J. 2009. Phospholipase C isozymes as effectors of Ras
9 superfamily GTPases. *J Lipid Res*. doi:10.1194/jlr.R800045-JLR200
10 Heasman SJ, Ridley AJ. 2008. Mammalian Rho GTPases: New insights into their
11 functions from in vivo studies. *Nat Rev Mol Cell Biol*. doi:10.1038/nrm2476
12 Henstidge CM, Balenga NAB, Ford LA, Ross RA, Waldhoer M, Irving AJ. 2009. The
13 GPR55 ligand L-α-lysophosphatidylinositol promotes RhoA-dependent Ca 2+
14 signaling and NFAT activation . *FASEB J*. doi:10.1096/fj.08-108670
15 Hogan PG, Chen L, Nardone J, Rao A. 2003. Transcriptional regulation by calcium,
16 calcineurin, and NFAT. *Genes Dev*. doi:10.1101/gad.1102703
17 Idevall-Hagren O, Dickson EJ, Hille B, Toomre DK, De Camilli P. 2012. Optogenetic
18 control of phosphoinositide metabolism. *Proc Natl Acad Sci U S A* **109**.

doi:10.1073/pnas.1211305109

Ikebe M, Hartshorne DJ. 1985. Phosphorylation of smooth muscle myosin at two distinct sites by myosin light chain kinase. *J Biol Chem*.

Irannejad R, Wedegaertner PB. 2010. Regulation of constitutive cargo transport from the trans-Golgi network to plasma membrane by Golgi-localized G protein βγ subunits. *J Biol Chem* **285**:32393–32404. doi:10.1074/jbc.M110.154963

Ishii T, Sato K, Kakumoto T, Miura S, Touhara K, Takeuchi S, Nakata T. 2015. Light generation of intracellular Ca2+ signals by a genetically encoded protein BACCS. *Nat Commun* **6**. doi:10.1038/ncomms9021

Jin P, Jan LY, Jan Y-N. 2020. Mechanosensitive Ion Channels: Structural Features Relevant to Mechanotransduction Mechanisms. *Annu Rev Neurosci*. doi:10.1146/annurev-neuro-070918-050509

Jin TG, Satoh T, Liao Y, Song C, Gao X, Kariya KI, Hu CD, Kataoka T. 2001. Role of the CDC25 Homology Domain of Phospholipase Cε in Amplification of Rap1-dependent Signaling. *J Biol Chem* **276**:30301–30307. doi:10.1074/jbc.M103530200

Kakumoto T, Nakata T. 2013. Optogenetic Control of PIP3: PIP3 Is Sufficient to Induce the Actin-Based Active Part of Growth Cones and Is Regulated via Endocytosis.

PLoS One **8**:1–17. doi:10.1371/journal.pone.0070861

Kalko EK V, Dukas R, Ratcliffe JM, Teeling EC, Haven N, Fattu JM, Bates ME, Simmons J a, Riquimaroux H, Surlykke A, Bouffard FH, Lee DN, Dear SP, Horiuchi TK, Krishnaprasad PS, Moss CF, Schuller G, Brudzynski SM, Syme D a, Hollingworth S, Lindstedt SL, Baylor SM, Mead a F, Rome LC, Goller F, Spierts ILY, Leeuwen JL Van, Schachat F, Rossmanith GH, Hoh JFY, Kelley DB, Vater M a, Zhao Y, Kalko EK V, Dukas R, Ratcliffe JM, Teeling EC, Haven N, Fattu JM, Bates ME, Simmons J a, Riquimaroux H, Surlykke A, Bouffard FH, Lee DN, Dear SP, Horiuchi TK, Krishnaprasad PS, Moss CF, Schuller G, Brudzynski SM, Syme D a, Hollingworth S, Lindstedt SL, Baylor SM, Mead a F, Rome LC, Goller F, Spierts ILY, Leeuwen JL Van, Schachat F, Rossmanith GH, Hoh JFY, Kelley DB, Vater M a. 2011. An Expanded Palette of Genetically. *Science (80-)* **557**:1888–1891. doi:10.1126/science.1208592

Kalwa H, Storch U, Demleitner J, Fiedler S, Mayer T, Kannler M, Fahlbusch M, Barth H, Smrcka A, Hildebrandt F, Gudermann T, Dietrich A. 2015. Phospholipase C Epsilon (PLCε) Induced TRPC6 Activation: A Common but Redundant Mechanism in Primary Podocytes. *J Cell Physiol* **230**:1389–1399. doi:10.1002/jcp.24883

1 Kelley GG, Reks SE, Ondrako JM, Smrcka A V. 2001. Phospholipase Cε: A novel Ras
2 effector. *EMBO J*. doi:10.1093/emboj/20.4.743
3 Kelley GG, Reks SE, Smrcka A V. 2004. Hormonal regulation of phospholipase Cε
4 through distinct and overlapping pathways involving G12 and Ras family G-
5 proteins. *Biochem J*. doi:10.1042/BJ20031370
6 Kennedy MJ, Hughes RM, Peteya LA, Schwartz JW, Ehlers MD, Tucker CL. 2010.
7 Rapid blue-light-mediated induction of protein interactions in living cells. *Nat*
8 *Methods* **7**:973–975. doi:10.1038/nmeth.1524
9 Kolch W. 2000. Meaningful relationships: the regulation of the Ras/Raf/MEK/ERK
10 pathway by protein interactions. *Biochem J*. doi:10.1042/bj3510289
11 Levskaya A, Weiner OD, Lim WA, Voigt CA. 2009. Spatiotemporal control of cell
12 signalling using a light-switchable protein interaction. *Nature*.
13 doi:10.1038/nature08446
14 Li Y, Brayden JE. 2017. Rho kinase activity governs arteriolar myogenic
15 depolarization. *J Cereb Blood Flow Metab* **37**:140–152.
16 doi:10.1177/0271678X15621069
17 Lopez I, Mak EC, Ding J, Hamm HE, Lomasney JW. 2001. A Novel Bifunctional
18 Phospholipase C That Is Regulated by Gα 12 and Stimulates the Ras/Mitogen-

activated Protein Kinase Pathway. *J Biol Chem* **276**:2758–2765. doi:10.1074/jbc.M008119200

Madukwe JC, Garland-Kuntz EE, Lyon AM, Smrcka A V. 2018. G protein subunits directly interact with and activate phospholipase C. *J Biol Chem*. doi:10.1074/jbc.RA118.002354

Malik S, De Rubio RG, Trembley M, Irannejad R, Wedegaertner PB, Smrcka A V. 2015. G protein βγ subunits regulate cardiomyocyte hypertrophy through a perinuclear Golgi phosphatidylinositol 4-phosphate hydrolysis pathway. *Mol Biol Cell* **26**:1188–1198. doi:10.1091/mbc.E14-10-1476

Martins M, Warren S, Kimberley C, Margineanu A, Peschard P, McCarthy A, Yeo M, Marshall CJ, Dunsby C, French PMW, Katan M. 2012. Activity of PLCε contributes to chemotaxis of fibroblasts towards PDGF. *J Cell Sci*. doi:10.1242/jcs.110007

Martz MK, Grabocka E, Beeharry N, Yen TJ, Wedegaertner PB. 2013. Leukemia-associated RhoGEF (LARG) is a novel RhoGEF in cytokinesis and required for the proper completion of abscission. *Mol Biol Cell* **24**:2785–2794. doi:10.1091/mbc.E12-07-0533

Mehta D, Ahmmed GU, Paria BC, Holinstat M, Voyno-Yasenetskaya T, Tiruppathi C,

1 Minshall RD, Malik AB. 2003. RhoA interaction with inositol 1,4,5-trisphosphate
2 receptor and transient receptor potential channel-1 regulates Ca2+ entry: Role in
3 signaling increased endothelial permeability. *J Biol Chem* **278**:33492–33500.
4 doi:10.1074/jbc.M302401200
5 Mitin N, Rossman KL, Der CJ. 2005. Signaling interplay in ras superfamily function.
6 *Curr Biol* **15**:563–574. doi:10.1016/j.cub.2005.07.010
7 Nash CA, Wei W, Irannejad R, Smrcka A V. 2019. Golgi localized βi-adrenergic
8 receptors stimulate golgi PI4P hydrolysis by PLCε to regulate cardiac hypertrophy.
9 *Elife* **8**:1–22. doi:10.7554/eLife.48167
10 O'Neill PR, Castillo-Badillo JA, Meshik X, Kalyanaraman V, Melgarejo K, Gautam N.
11 2018. Membrane Flow Drives an Adhesion-Independent Amoeboid Cell Migration
12 Mode. *Dev Cell* **46**:9-22.e4. doi:10.1016/j.devcel.2018.05.029
13 Pertz O, Hodgson L, Klemke RL, Hahn KM. 2006. Spatiotemporal dynamics of RhoA
14 activity in migrating cells. *Nature* **440**:1069–1072. doi:10.1038/nature04665
15 Reid T, Furuyashiki T, Ishizaki T, Watanabe G, Watanabe N, Fujisawa K, Morii N,
16 Madaule P, Narumiya S. 1996. Rhotekin, a new putative target for Rho bearing
17 homology to a serine/threonine kinase, PKN, and rhophilin in the Rho-binding
18 domain. *J Biol Chem* **271**:13556–13560. doi:10.1074/jbc.271.23.13556

1 Schindelin J, Arganda-Carreras I, Frise E, Kaynig V, Longair M, Pietzsch T, Preibisch
2 S, Rueden C, Saalfeld S, Schmid B, Tinevez JY, White DJ, Hartenstein V, Eliceiri
3 K, Tomancak P, Cardona A. 2012. Fiji: An open-source platform for biological-
4 image analysis. *Nat Methods*. doi:10.1038/nmeth.2019
5 Seifert JP, Zhou Y, Hicks SN, Sondek J, Harden TK. 2008. Dual activation of
6 phospholipase C-ε by rho and ras GTPases. *J Biol Chem*.
7 doi:10.1074/jbc.M805038200
8 Shiwarski DJ, Darr M, Telmer CA, Bruchez MP, Puthenveedu MA. 2017. PI3K class II
9 α regulates δ-opioid receptor export from the trans-Golgi network. *Mol Biol Cell*
10 **28**:2202–2219. doi:10.1091/mbc.E17-01-0030
11 Smrcka A V., Brown JH, Holz GG. 2012. Role of phospholipase Cε in physiological
12 phosphoinositide signaling networks. *Cell Signal*.
13 doi:10.1016/j.cellsig.2012.01.009
14 Song C, Hu CD, Masago M, Kariya KI, Yamawaki-Kataoka Y, Shibatohge M, Wu D,
15 Satoh T, Kataoka T. 2001. Regulation of a Novel Human Phospholipase C, PLCε,
16 through Membrane Targeting by Ras. *J Biol Chem*. doi:10.1074/jbc.M008324200
17 Stauffer TP, Ahn S, Meyer T. 1998. Receptor-induced transient reduction in plasma
18 membrane Ptdlns(4,5)P2 concentration monitored in living cells. *Curr Biol* **8**:343–

346. doi:10.1016/s0960-9822(98)70135-6

Strickland D, Lin Y, Wagner E, Hope CM, Zayner J, Antoniou C, Sosnick TR, Weiss EL, Glotzer M. 2012. TULIPs: Tunable, light-controlled interacting protein tags for cell biology. *Nat Methods* **9**:379–384. doi:10.1038/nmeth.1904

Team RDC. 2016. R: A language and environment for statistical computing.

Tischer D, Weiner OD. 2014. Illuminating cell signalling with optogenetic tools. *Nat Rev Mol Cell Biol* **15**:551–558. doi:10.1038/nrm3837

Toettcher JE, Voigt CA, Weiner OD, Lim WA. 2011. The promise of optogenetics in cell biology: Interrogating molecular circuits in space and time. *Nat Methods* **8**:35–38. doi:10.1038/nmeth.f.326

Toettcher JE, Weiner OD, Lim WA. 2013. Using optogenetics to interrogate the dynamic control of signal transmission by the Ras/Erk module. *Cell*. doi:10.1016/j.cell.2013.11.004

Valon L, Marín-Llauradó A, Wyatt T, Charras G, Trepat X. 2017. Optogenetic control of cellular forces and mechanotransduction. *Nat Commun* **8**. doi:10.1038/ncomms14396

Wagner E, Glotzer M. 2016. Local RhoA activation induces cytokinetic furrows independent of spindle position and cell cycle stage. *J Cell Biol* **213**:641–649.

1 doi:10.1083/jcb.201603025

2 Weng Y, Yan F, Chen R, Qian M, Ou Y, Xie S, Zheng H, Li J. 2018. PIEZO channel

3 protein naturally expressed in human breast cancer cell MDA-MB-231 as probed

4 by atomic force microscopy. *AIP Adv*. doi:10.1063/1.5025036

5 Wennerberg K, Rossman KL, Der CJ. 2005. The Ras superfamily at a glance. *J Cell Sci*

6 **118**:843–846. doi:10.1242/jcs.01660

7 Wilsher NE, Court WJ, Ruddle R, Newbatt YM, Aherne W, Sheldrake PW, Jones NP,

8 Katan M, And SAE, Raynaud FI, Therapeutics E. 2007. The Phosphoinositide-

9 Specific Phospholipase C Inhibitor Conjugates with Common Components of Cell

10 Culture. *Drug Metab Dispos*. doi:10.1124/dmd.106.014498.activity

11 Wing MR, Houston D, Kelley GG, Der CJ, Siderovski DP, Harden TK. 2001.

12 Activation of Phospholipase C-ε by Heterotrimeric G Protein βγ-Subunits. *J Biol*

13 *Chem*. doi:10.1074/jbc.C100574200

14 Wing MR, Snyder JT, Sondek J, Harden TK. 2003. Direct Activation of Phospholipase

15 C-ε by Rho. *J Biol Chem* **278**:41253–41258. doi:10.1074/jbc.M306904200

16 Wu YI, Frey D, Lungu OI, Jaehrig A, Schlichting I, Kuhlman B, Hahn KM. 2009. A

17 genetically encoded photoactivatable Rac controls the motility of living cells.

18 *Nature* **461**:104–108. doi:10.1038/nature08241

Xiang SY, Ouyang K, Yung BS, Miyamoto S, Smrcka A V., Chen J, Brown JH. 2013. PLCε, PKD1, and SSH1L transduce RhoA signaling to protect mitochondria from oxidative stress in the heart. *Sci Signal*. doi:10.1126/scisignal.2004405

Xu FP, Chen MS, Wang YZ, Yi Q, Lin SB, Chen AF, Luo JD. 2004. Leptin induces hypertrophy via endothelin-1-reactive oxygen species pathway in cultured neonatal rat cardiomyocytes. *Circulation*. doi:10.1161/01.CIR.0000140766.52771.6D

Yu S, Choi W Il, Choi YJ, Kim HY, Hildebrandt F, Gee HY. 2020. PLCE1 regulates the migration, proliferation, and differentiation of podocytes. *Exp Mol Med*. doi:10.1038/s12276-020-0410-4

Zago G, Veith I, Singh MK, Fuhrmann L, De Beco S, Remorino A, Takaoka S, Palmeri M, Berger F, Brandon N, El Marjou A, Vincent-Salomon A, Camonis J, Coppey M, Parrini MC. 2018. Ralb directly triggers invasion downstream ras by mobilizing the wave complex. *Elife* **7**:1–23. doi:10.7554/eLife.40474

Zhang L, Malik S, Pang J, Wang H, Park KM, Yule DI, Blaxall BC, Smrcka A V. 2013. Phospholipase Cε Hydrolyzes Perinuclear Phosphatidylinositol 4-Phosphate to Regulate Cardiac Hypertrophy. *Cell* **153**:216–227. doi:10.1016/j.cell.2013.02.047

Zhao Y, Araki S, Wu J, Teramoto T, Chang YF, Nakano M, Abdelfattah AS, Fujiwara M, Ishihara T, Nagai T, Campbell RE. 2011. An expanded palette of genetically

1 encoded Ca2+ indicators. *Science (80-)*. doi:10.1126/science.1208592

2 Zhu L, Qi XY, Aoudjit L, Mouawad F, Baldwin C, Nattel S, Takano T. 2013. Nuclear

3 factor of activated T cells mediates RhoA-induced fibronectin upregulation in

4 glomerular podocytes. *Am J Physiol - Ren Physiol*.

5 doi:10.1152/ajprenal.00495.2012

6

7

1 **Figure legends**

2

3 **Figure 1. Development of an optogenetic tool to control RhoA activity. (A)** Schematic
4 of opto-RhoA. Spatiotemporal control of RhoA activity is achieved using an optogenetic
5 probe to recruit RhoA-specific GEF LARG to the PM. An iLID molecule is anchored to
6 the PM via the CAAX motif, while a protein consisting of SspB fused to the DH domain
7 of LARG is distributed throughout the cytosol. When irradiated with blue-light, iLID
8 undergoes a conformational change exposing a binding site for SspB, and driving LARG-
9 DH to the PM, where it activates RhoA. **(B)** Representative images of HeLa cells
10 expressing opto-RhoA before (458 nm light OFF) and after (458 nm light ON) light
11 irradiation with a 458 nm laser. **(C)** Representative images of HeLa cells expressing opto-
12 RhoA and mCherry-$RBD_{rhotekin}$. Opto-RhoA was locally activated with a 458 nm laser
13 within 300–600 sec every 20 sec. Blue boxes in images indicate the activated area, and
14 lower panels showed high magnification images for this area. (**D, E**) Quantification of
15 local intensity increases of mVenus-SspB-LARG-DH (**D**) and mCherry-$RBD_{rhotekin}$ (**E**)
16 from the images shown in **(C)**. Activation period is indicated by a blue background.
17 Experiments were repeated seven times.

18

1 **Figure 2. RhoA activation induces intracellular calcium transients in various cell**
2 **types. (A, B)** Screening for small GTPases that induce intracellular calcium mobilization.
3 RPE1 **(A)** and HeLa **(B)** cells transiently express opto-GTPases, and the calcium reporter
4 R-GECO1 were observed with confocal microscopy in Leibovitz's L-15 medium. Opto-
5 GTPases were activated by a multi-argon 458 nm laser every 10 sec for 2 minutes.
6 Percentages of cells exhibiting intracellular calcium transients ($F/F_0 > 2$) in response to
7 opto-GTPases activation are shown. Data are presented as means ± SEM from more than
8 three independent experiments. In total, >150 cells were analyzed for each photoswitch.
9 **(C)** Representative images of RPE1 cells expressing opto-RhoA or GEF-inactive mutant
10 opto-RhoA^{YA} and calcium reporter, R-GECO1. From time 0 sec, opto-RhoA was
11 activated by a multi-argon 458 nm laser every 10 sec. Scale bar = 20 μm. **(D)** Intensity
12 changes of R-GECO1 during RhoA activation in various cell types. Only cells exhibiting
13 intracellular calcium transients were analyzed. Data are presented as means ± SEM from
14 indicated numbers of cells.
15
16 **Figure 3. Mechanisms of intracellular calcium transients induced by RhoA are**
17 **different among cell types.** RPE1 (**A**), HeLa (**B**), MDCK (**C**), and HEK293T (**D**) cells
18 expressing opto-RhoA and R-GECO1 were treated with DMSO, 50 μM Y-27632 (ROCK

inhibitor), 20 μM Blebbistatin (myosin II inhibitor), 10 μM SKF96365, 100 μM 2-APB (calcium channel inhibitors), or 10 μM U73122 (PLC inhibitor) and were observed using confocal microscopy (see Figure 2). Leibovitz's L-15 medium and Ringer's solution with or without Ca^{2+} were used for the experiments. Percentages of cells exhibiting intracellular calcium transients (F/F_0 >2) in response to RhoA activation are shown. Data are shown as means ± SEM from more than three independent experiments. In total, >200 cells were analyzed for each condition. ***, $p < 0.001$; **, $p < 0.01$; and n.s., not significant; two-tailed unpaired Student's t-test.

Figure 4. RhoA directly activates PLCε and induces intracellular calcium transients in RPE1 and HeLa cells. (A) RPE1 and HeLa cells were treated with PLCε-specific or control siRNAs for 48 h. Proteins in total cell extracts were separated with SDS-PAGE and immunoblotted with anti-PLCε and anti-vinculin antibodies. Vinculin was used as a loading control. **(B)** siRNA-mediated PLCε-depleted RPE1 and HeLa cells express opto-RhoA and R-GECO1 (see Figure 2). **(C)** Schematic of mouse PLCε (msPLCε). CDC25, CDC25 homology guanine nucleotide exchange factor (GEF) domain; PH, pleckstrin homology domain; EF, EF-hand motif; X and Y, X and Y domains fold to form the catalytic core of the phospholipase; C2, C2 domain; RA, ras (RA) association homology

domain. **(D)** Proteins in total extracts from HEK293T cells expressing ECFP, msPLCε-ECFP wild-type (WT), or indicated msPLCε-ECFP mutants were separated with SDS-PAGE and immunoblotted with anti-GFP and anti-β-actin antibodies. β-actin was used as a loading control. **(E)** siRNA-mediated PLCε-depleted HeLa cells transiently expressing ECFP, msPLCε-ECFP WT or indicated msPLCε-ECFP mutants, and R-GECO1 (see Figure 2). Data are presented as means ± SEM from three independent experiments. In total, >150 cells were analyzed for each condition. ***, $p < 0.001$; and n.s., not significant; two-tailed unpaired Student's t-test.

Figure 5. RhoA activates PLCε at the PM and marginally affects membrane phosphoinositide dynamics. (A) Schematic of opto-RhoA-TGN and opto-RhoA-Golgi. TGN, trans-Golgi network localized N-terminus transmembrane domain of 2,6-sialyltransferase; KDELr DN, dominant-negative (DN) KDELr D193N. **(B)** Representative images of HeLa cells expressing opto-RhoA-TGN or opto-RhoA-Golgi before (458 nm light OFF) and after (458 nm light ON) light irradiation with a 458 nm laser. **(C)** RPE1 and HeLa cells expressing opto-RhoA, opto-RhoA-TGN, or opto-RhoA-Golgi, and R-GECO1 (see Figure 2). Data are presented as means ± SEM from three independent experiments (in total >150 cells were analyzed for each photoswitch). ***,

1 $p < 0.001$; **, $p < 0.01$; and n.s., not significant; one-way ANOVA and Tukey's test. **(D)**

2 Schematic of opto-5-ptase. OCRLcat, inositol 5-phosphatase catalytic domain of OCRL.

3 **(E)** Representative images of cells expressing opto-5-ptase or opto-RhoA and PI(4,5)P_2

4 marker, mCherry-PLCδ-PH, before and after 458 nm light irradiation. **(F)** Quantification

5 of cytosolic mCherry-PLCδ-PH intensity. HeLa cells expressing indicated photoswitches

6 (opto-5-ptase or opto-RhoA), and markers (mCherry-PLCδ-PH or mCherry alone) were

7 observed by confocal microscopy with or without 458 nm light irradiation every 10 s (458

8 nm ON or 458 nm OFF, respectively). Cells were first observed without 458 nm light

9 irradiation, and then the same cells were observed with light irradiation. Data are

10 presented as means ± SEM from the indicated number of experiments.

11

12 **Figure 6. Optogenetic RhoA activation induces intracellular calcium signaling (A)**

13 Time-lapse imaging of NFAT-mCherry translocation in HeLa cells. Cells expressing opto-

14 RhoA and NFAT-mCherry were observed by confocal microscopy with a 458 nm laser

15 irradiation every 10 sec. Bar = 20 μm. **(B)** Time-course of the relative fluorescence

16 intensity of nuclear NFAT-mCherry. Cells indicated in **A** were analyzed. **(C, D)** Nuclear

17 to cytosol ratio (**C**) and changes of this ratio (**D**) of NFAT-mCherry before (dark) and after

18 5 min (Lit). HeLa cells were treated with individual siRNA duplexes for 48 h and

transiently expressed opto-RhoA and NFAT-mCherry. Data from three independent experiments is shown in box-and-whisker plots. Boxes represent the first to third quartiles (interquartile range: IQR). The horizontal line inside the box represents the median—vertical lines above and below the box span 1.5×IQR. Dots represent outliers that are above or below 1.5×IQR. In total, 61, 58, and 72 cells treated with si control, si PLCε seq1, and seq3 were analyzed, respectively. ***, $p < 0.001$; **, $p < 0.01$; and n.s., not significant; two-tailed paired Student's t-test (**C**) and one-way ANOVA followed by Wilcoxon signed-rank test (**D**).

Figure 7. Summary of the study. See details in the discussion.

Inaba et al., Figure 1

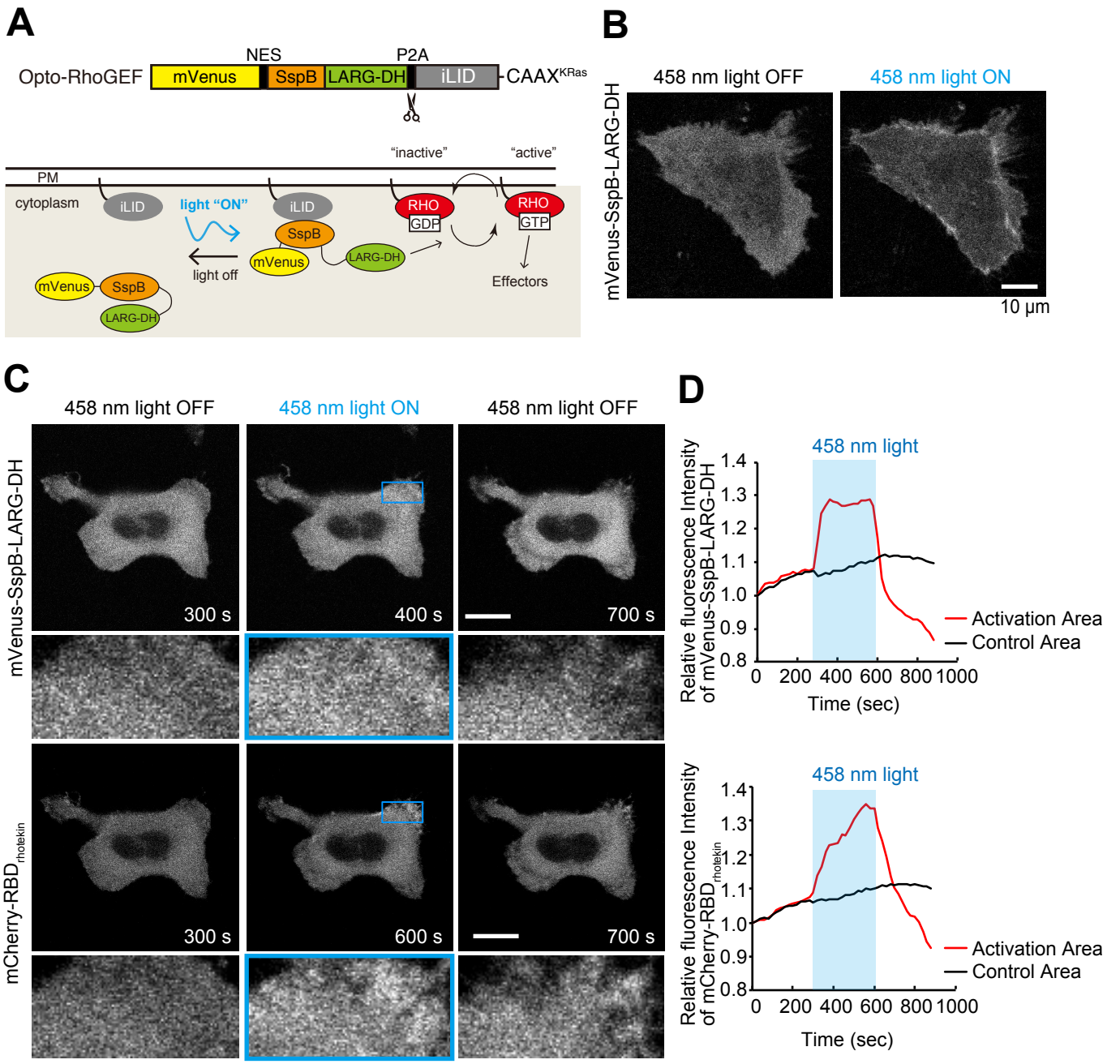

Inaba et al., Figure 2

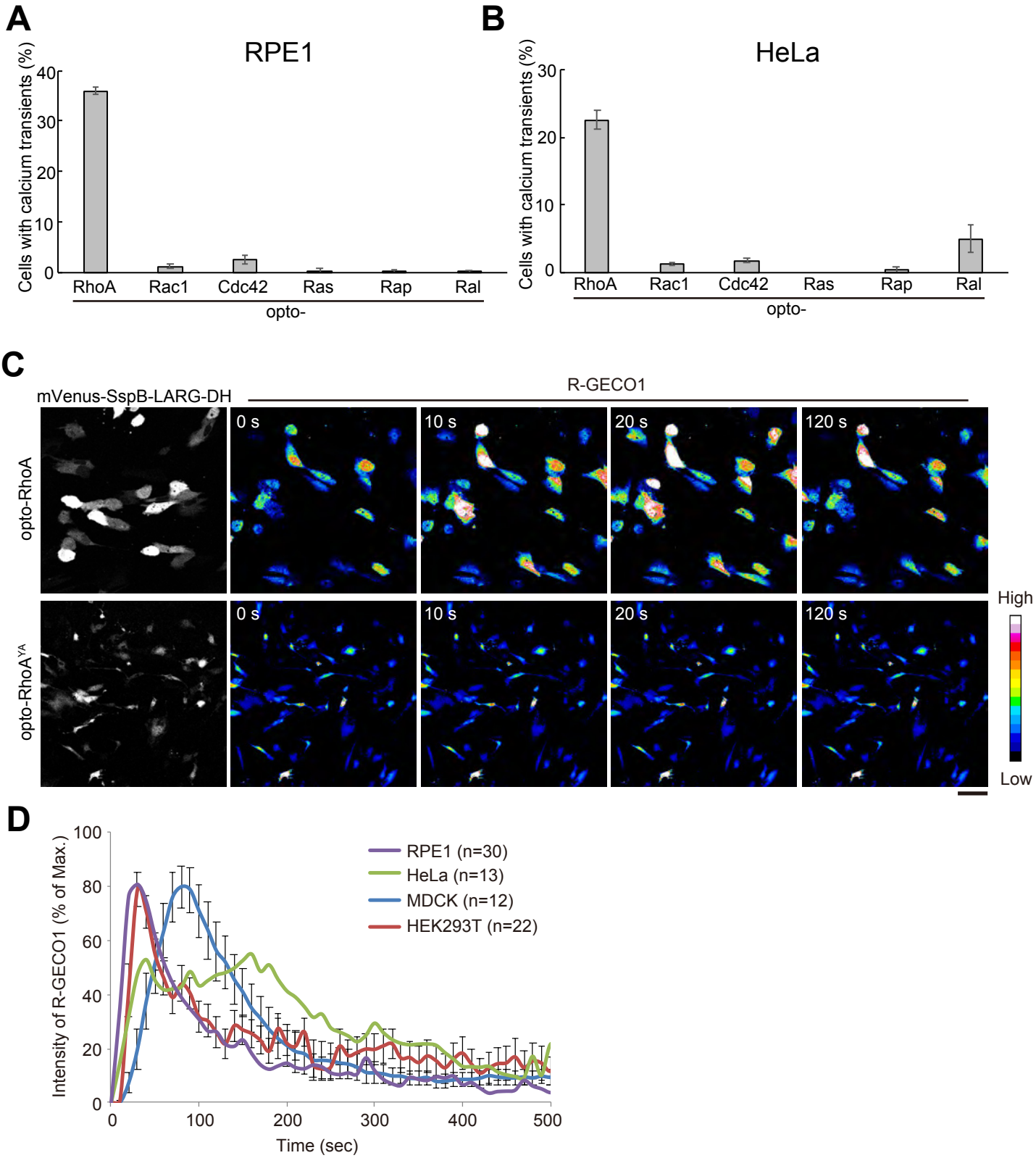

Inaba et al., Figure 3

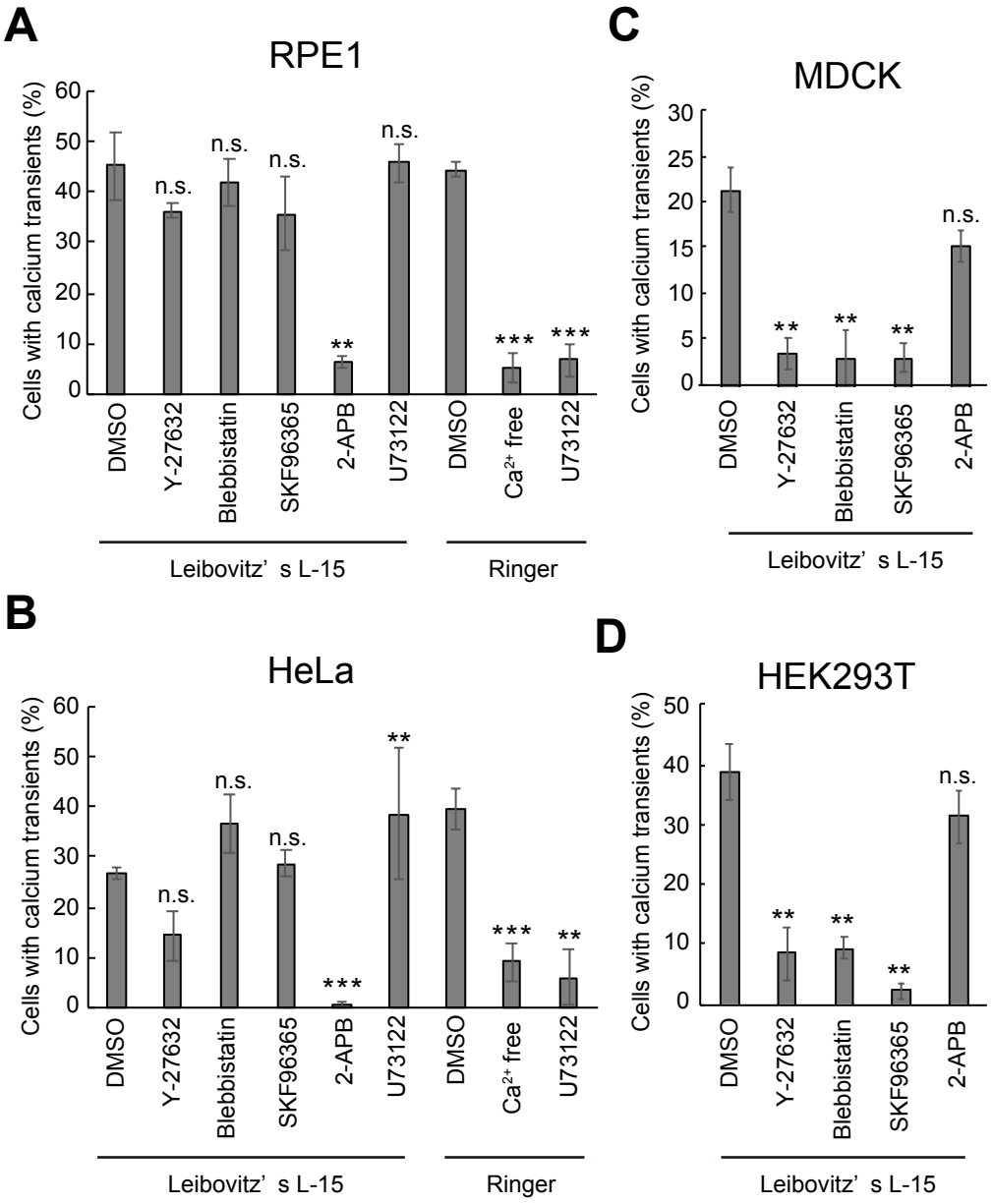

Inaba et al., Figure 4

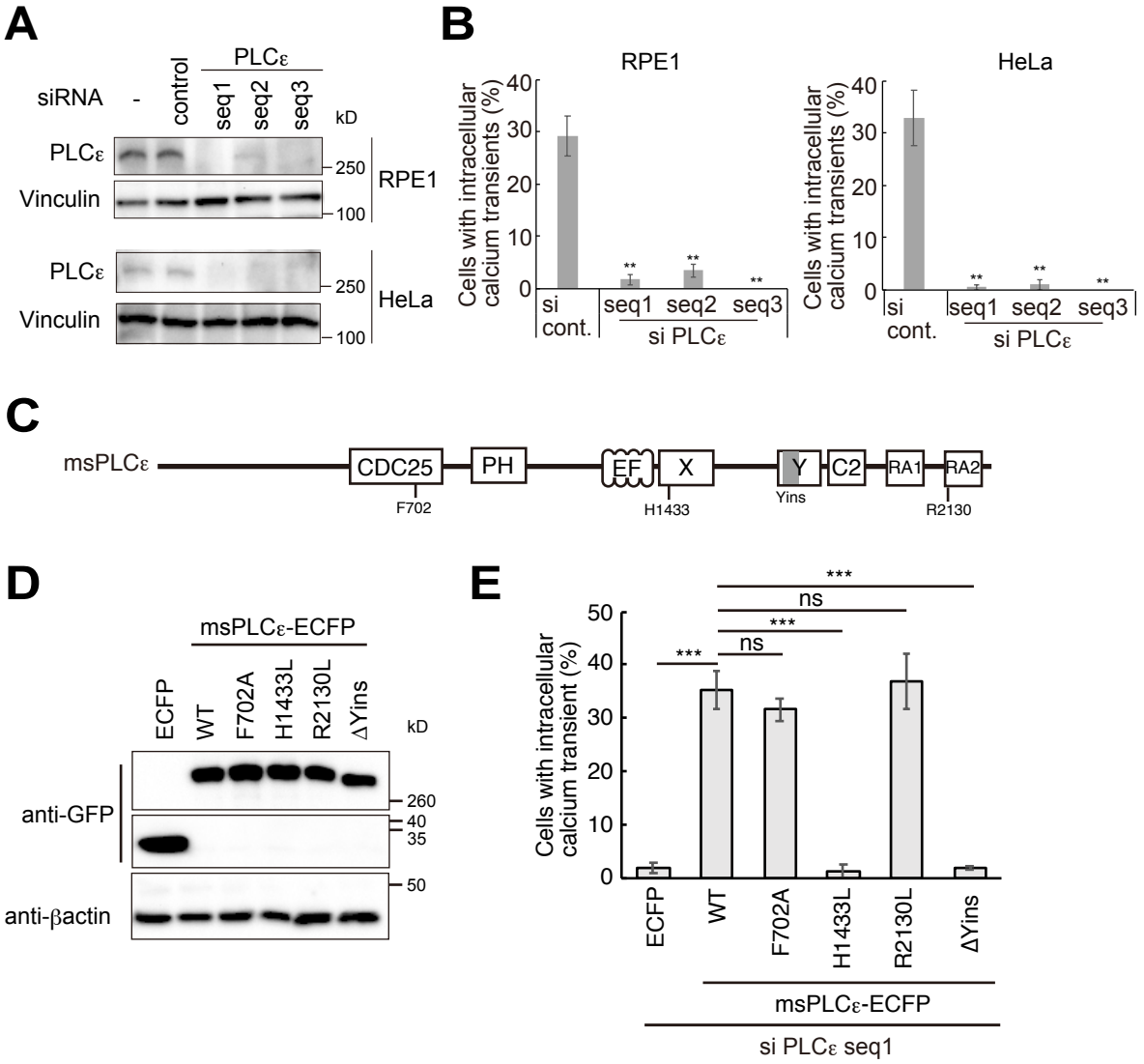

Inaba et al., Figure 5

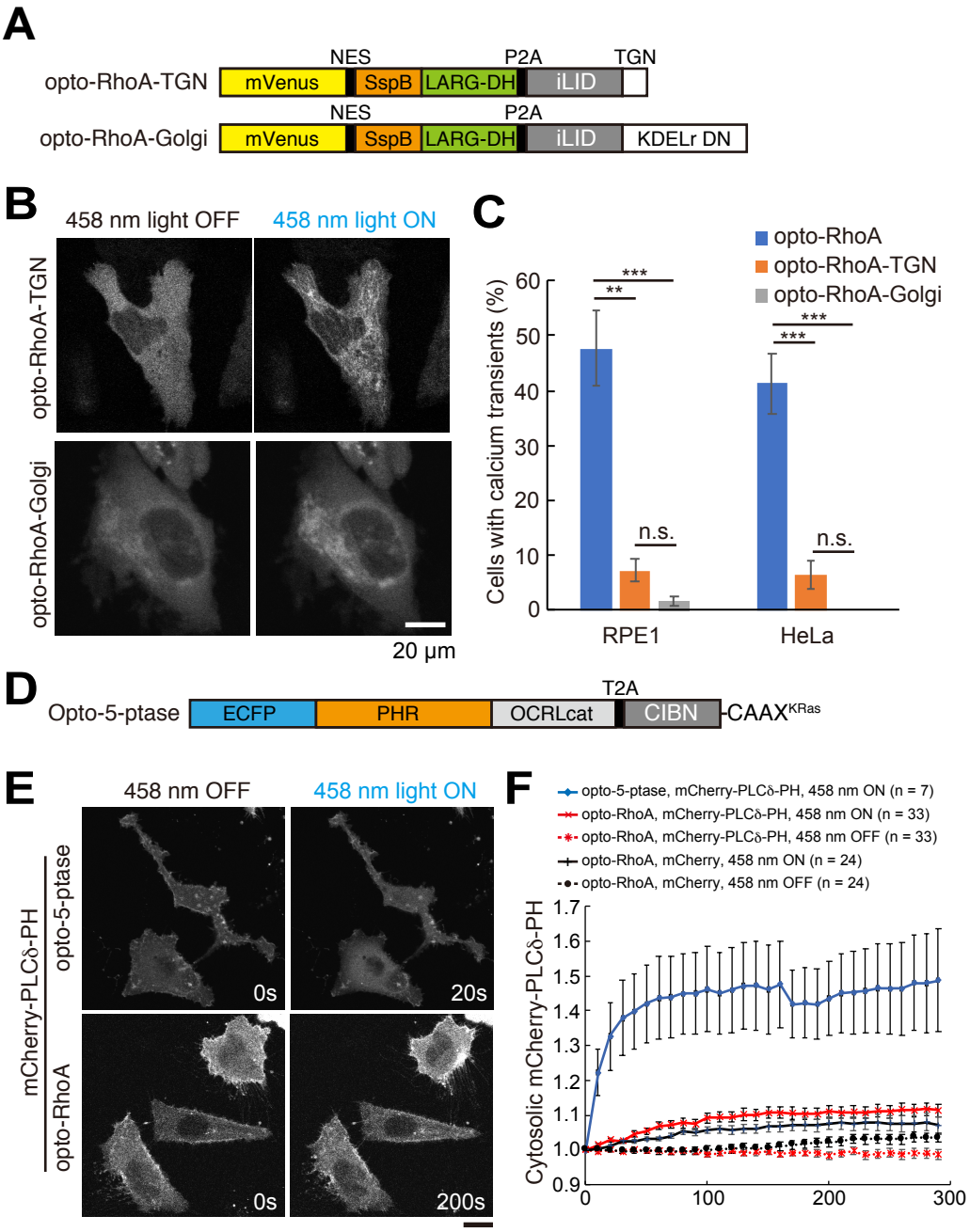

Inaba et al., Figure 6

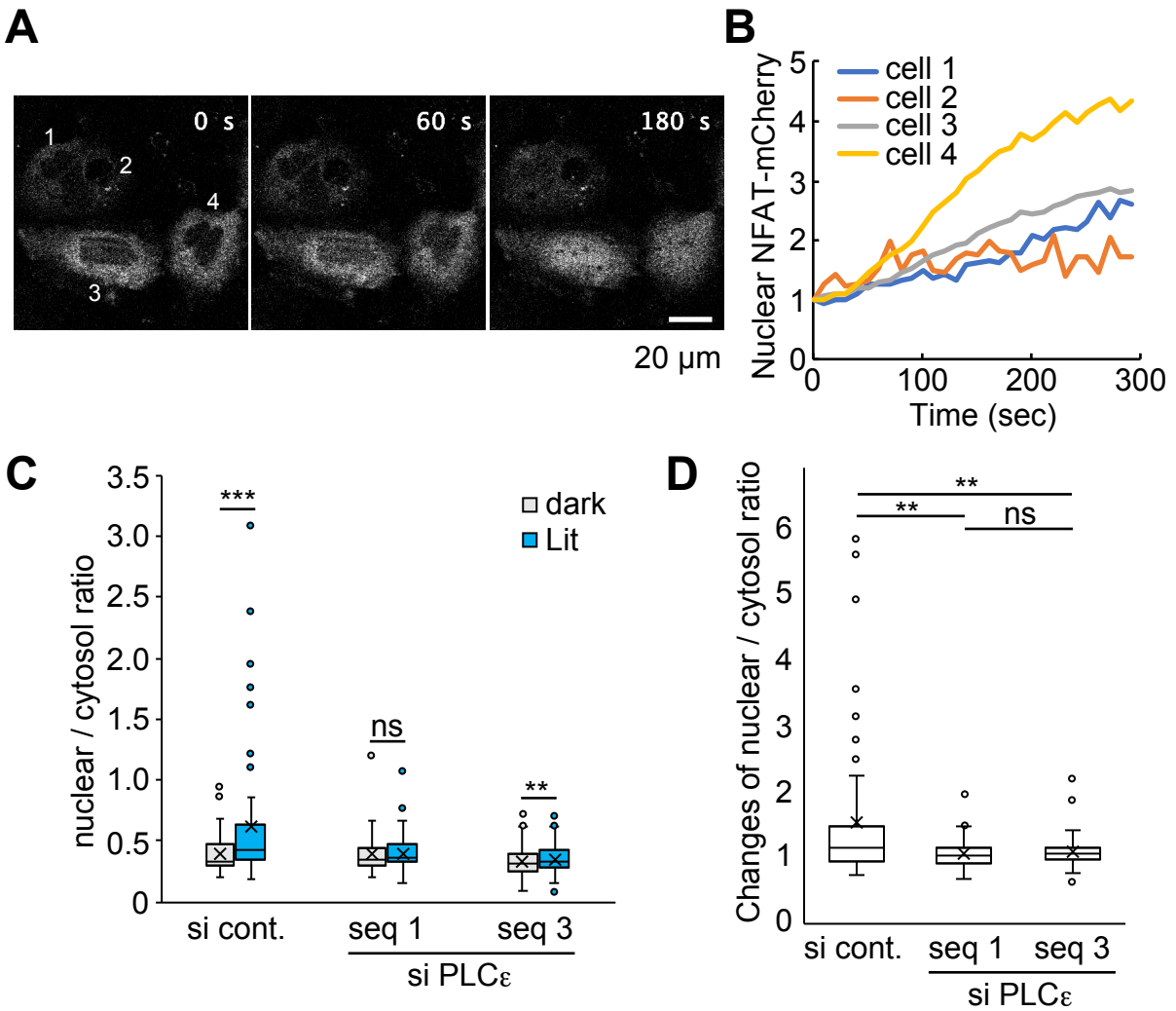
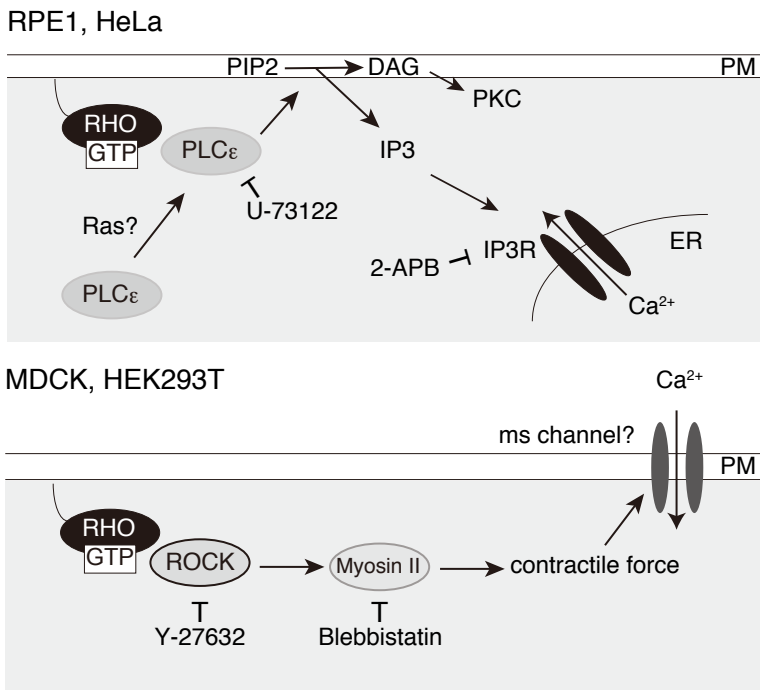
Inaba et al., Figure 7